IOPscience iopscience.iop.org

Home Search Collections Journals About Contact us My IOPscience

Colloidal systems: a promising material class for tailoring sound propagation at high frequencies

This article has been downloaded from IOPscience. Please scroll down to see the full text article.

2008 J. Phys.: Condens. Matter 20 404203

(http://iopscience.iop.org/0953-8984/20/40/404203)

View the table of contents for this issue, or go to the journal homepage for more

Download details:
IP Address: 129.252.86.83
The article was downloaded on 29/05/2010 at 15:31

Please note that terms and conditions apply.

IOP PUBLISHING JOURNAL OF PHYSICS: CONDENSED MATTER

J. Phys.: Condens. Matter **20** (2008) 404203 (9pp) doi:10.1088/0953-8984/20/40/404203

Colloidal systems: a promising material class for tailoring sound propagation at high frequencies

T Still[1], W Cheng[1], M Retsch[1], U Jonas[1,2] and G Fytas[1,2,3]

[1] Max Planck Institute for Polymer Research, Ackermannweg 10, D-55128 Mainz, Germany
[2] FORTH-Institute of Electronic Structure and Laser, PO Box 1527, GR-71110 Heraklion, Greece
[3] Department of Materials Science and Technology, University of Crete, Heraklion, Greece

E-mail: fytas@mpip-mainz.mpg.de

Received 26 April 2008
Published 10 September 2008
Online at stacks.iop.org/JPhysCM/20/404203

Abstract

In this paper we report on the phononic properties of mesoscopic colloidal materials. Using high resolution Brillouin light scattering (BLS) the resonance modes of submicron particles as well as the dispersion relations of their ordered assemblies in a liquid matrix are studied. Two different kinds of very recently realized acoustic bandgaps are presented. In colloidal mixtures, the particle acoustic resonances are independent of composition.

(Some figures in this article are in colour only in the electronic version)

1. Introduction

The first papers on photonic effects by Yablonovitch [1] and John [2] in 1987 stimulated over the years much theoretical and experimental work on the propagation of electromagnetic waves through appropriately structured materials and subsequently led to the birth of the new research field 'photonic crystals' [3]. The tremendous interest in photonic crystals with specially designed periodic variations in dielectric constant largely originates from their display of propagation bandgaps for light. The appearance of bandgaps makes an advanced control over light propagation possible and permits as well a series of novel optical phenomena such as slowing and localization of light and negative refraction [3]. Soon after the discovery of photonic crystals, it was found that, in analogy to electromagnetic waves, bandgaps also exist for the propagation of acoustic waves, and the so-called phononic crystals [4–10] are the elastic analogue of photonic crystals, replacing the role of the dielectric constant by the elastic parameters and density. Such an analogy exists as a consequence of the common origin of the bandgaps in both cases, i.e. the destructive interference of Bragg diffracted waves in periodic structures [11, 12], and hence these gaps are also termed as 'Bragg gaps'. However, the different nature of electromagnetic and acoustic waves also guarantees the existence of some important differences between photonic and phononic phenomena. Unlike electromagnetic radiation which is characterized as transverse waves, acoustic waves in general are full vector waves with both longitudinal and transverse polarizations, and their propagation depends additionally on the material density. Even for a homogeneous and isotropic medium, the acoustic wave propagation is governed by three parameters, the two Lamé coefficients and density, in contrast to the single parameter, the dielectric constant, that determines the propagation of light. Evidently, the phononic phenomena are anticipated to be more complex and rich.

For phononic crystals, the band diagram depends on several parameters such as the elastic constants and density of the component materials, symmetry of the lattice, shape of the inclusions and the filling fraction. The width of the bandgap generally increases with the contrast between the densities and sound phase velocities of the component materials, and the centre of the gap can be tuned by changing the lattice parameter [4, 5]. The search for phononic structures started with two theoretical works [4, 5] in 1993 which predicted the existence of phononic bandgaps in periodic two-dimensional (2D) elastic composites of parallel cylinders embedded in a host matrix. The experimental verification of phononic bandgaps followed a few years later, realized in metallic macrostructures with gaps at sonic or ultrasonic

 © 2008 IOP Publishing Ltd Printed in the UK

frequencies [6, 7, 13, 9]. Further explorations also revealed a number of peculiar phenomena with potential applications associated with acoustic wave propagation including the tunnelling effect [14], negative refraction and focusing [15], double refraction, etc [16].

Theoretical calculation of the phononic band diagram requires no specification of the lattice constant of the structure or the corresponding wave frequencies as long as the crystal is defined by the same set of frequency-independent elastic parameters. In other words, a fundamental length scale does not exist for phononic phenomena, which is a direct consequence of the invariance of the wave equation of elasticity under the simultaneous transformation of space coordinates and frequency. However, acoustic waves of different frequencies do bear distinct characteristics, particularly where their applications are concerned, and therefore in practice the frequency range of the waves of interest constitutes an important consideration. Recently, growing attention has been paid to hypersonic (GHz) phononic crystals and the first experimental observations of the hypersonic 'Bragg gaps' have been lately reported in three-dimensional (3D) colloidal crystals made by self-assembly [17] and in 2D polymeric porous structures with hexagonal symmetry created by laser interference lithography [18]. Hypersonic waves, owing to their high frequencies, display certain unique features that are not possessed by ordinary acoustic waves, such as being thermally excited, acting as the main heat carrier in dielectrics and interacting with electrons and photons in a rich manner. Consequently, hypersonic crystals with the potential to mould the flow of hypersound may be utilized to achieve high-level control over many important physical processes involving heat transport and complex phonon–photon or phonon–electron couplings. A detailed understanding of phonon propagation in hypersonic crystals thus becomes important.

The fabrication of hypersonic crystals, compared with their sonic and ultrasonic counterparts, is much more demanding as the dimension typifying the structure has to be scaled from macroscopic down to submicron scales. On the other hand, advances in relevant nanofabrication, partially driven by the desire to create various photonic structures of similar dimensions, has offered some available means to achieve such a purpose including, for example, holographic interference lithography [19], direct laser-writing [20], two-photon polymerization [21] and self-assembly [22]. Colloidal superstructures, self-assembled from colloidal particles, represent a promising material class for phononic applications. The maturation of colloidal science enables the preparation of colloidal particles with well-defined size and shape for a great many materials ranging from organic to inorganic, thus providing abundant building blocks with varied elastic properties. The progress in colloidal particle self-assembly allows easy and cheap fabrication of large-area high-quality single-crystalline 2D and 3D crystals as well as non-crystalline structures. The appearance of binary [23] and ternary [24] crystals further enriches the available structure types. By filling the interstitials between the colloidal particles with different materials, additional freedom in elastic parameters of the system is provided. Moreover, in most cases the colloidal particles possess a spherical shape due to the surface tension effect, thus representing a strong scattering unit when the elastic contrast between the particle and the surroundings becomes large, which may cause additional gap formation with an origin different from Bragg diffraction, as we will encounter later [25].

The experimental exploration of hypersonic crystals, however, faces an additional challenge in monitoring the phonons in such small structures. Apparently, the commonly used sonic and ultrasonic transmission techniques for macroscopic sized structures cease to work. It has been demonstrated that Brillouin light scattering (BLS), which takes advantage of the inelastic scattering of photons by thermally excited high frequency phonons, represents a powerful tool to record the phonon dispersion relation in hypersonic crystals. In this paper, we will report the results from our group on the BLS investigation of phononic properties of colloidal superstructures fabricated by self-assembly of submicron particles. This paper is organized as follows. First we introduce the relevant experimental aspects embodying BLS and colloidal crystal fabrication. Then we focus on the elastic properties of individual colloidal particles. Our subsequent attention is on phonon dispersion behaviour in crystals consisting of colloidal particles embedded in fluids. We demonstrate the existence of a hypersonic 'Bragg gap' and present the evidence of additional gap formation of non-Bragg type when the elastic contrast between the particle and fluid increases. Next, the fabrication of colloidal hybrid systems is utilized to confirm that the opening of the additional gap relates to the particle local resonances and the so-called hybridization gap is inert to the colloidal structure. We end the paper by providing some perspectives.

2. Brillouin light scattering

BLS is the inelastic scattering of monochromatic laser light by phonons in the GHz frequency range. The required high resolution is obtained by the use of multipass tandem Fabry–Perot interferometers schematically shown in figure 1. In BLS spectroscopy of transparent samples, the desired dispersion relations are obtained by recording the phonon frequencies as a function of the scattering wavevector **q**, which varies with the scattering angle. However, in samples exhibiting strong multiple light scattering, as for the dry colloidal crystals (opals), **q** is ill defined and hence **q**-dependent acoustic-like modes become inaccessible. Though localized in space, **q**-independent modes can be recorded in the BLS spectrum as was demonstrated for submicron colloidal silica [26] and polymer crystals [27]. These **q**-independent frequencies have been identified as the resonance modes of the individual colloidal particles, i.e. BLS can record numerous thermally excited elastic resonances in one measurement. These eigenfrequencies are uniquely defined by the geometrical and elastic characteristics of the particles. Based on these data, the elastic properties of the materials can be calculated at nanoscale. Thus the combination of **q**-independent BLS spectroscopy of multiply light scattering

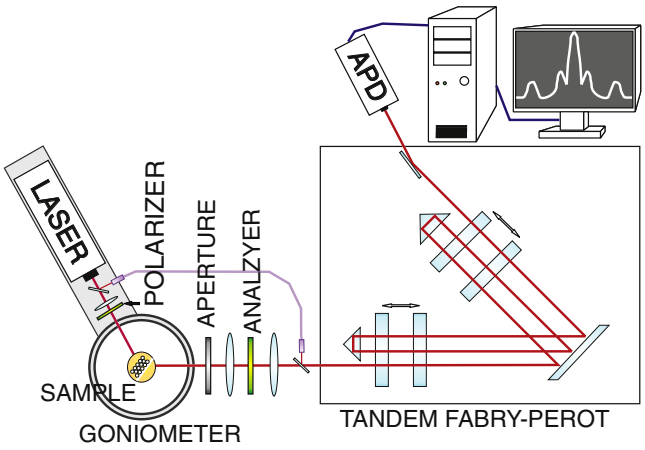

Figure 1. BLS set-up with six-pass tandem Fabry–Perot interferometer. Electronic stabilization over days to weeks is achieved by permanent compensation using a diverted part of the unscattered light as the reference beam. The goniometer allows us to record dispersion relations with continuous **q** range. For the eigenmode spectra the scattering angle is not relevant.

(opaque) samples and the dispersion relations from the **q**-dependent BLS spectroscopy on transparent samples is a powerful methodology to investigate the elastic behaviour of nanostructured materials.

3. Colloidal crystals

The assembly of colloids into well-defined coherent structures commonly occurs under the influence of external fields, e.g. gravitational sedimentation [28], electrophoretic deposition [29] or vertical deposition either by evaporation [30] or lifting the substrate [31].

In the vertical lifting deposition method, upon immersion of a hydrophilic substrate into a colloidal dispersion a meniscus with the substrate is formed. Evaporation takes place at the three phase contact lines (air, dispersion and substrate), which causes a solvent flux towards the meniscus. Thus, colloidal particles are constantly transported with the liquid to the crystallization front. An interplay of long-range attractive and short-range repulsive forces causes the self-assembly of the colloidal material into a face-centred cubic (fcc) or hexagonally close packed (hcp) crystal [32, 33]. In order to control the thickness of such a colloidal crystal—a critical parameter for further use in ensuing applications—the substrate is withdrawn from the dispersion at a certain speed under given environmental parameters such as temperature and humidity. Besides the fabrication of such 'simple' colloidal crystals, also more complex systems like binary [23, 34] and ternary colloidal crystals [24] were demonstrated. The colloidal crystals that are the topic of this paper are produced using an enhanced vertical lifting apparatus [35].

Alongside with this research, the counterparts—colloidal glasses [36, 37]—comprising two distinct, monodisperse latex particles have also already been developed [25]. Doping of the colloidal crystal with removable moieties (sacrificial templates) opens a pathway to the designed introduction of defects, which are highly interesting with respect to their contribution to phononic properties. At the same time, colloidal crystals and glasses serve as templates for the fabrication of so-called inverse opals [38]. These materials exhibit an interconnected 3D network with high surface area, since the constituent spheres of the colloidal crystals have been removed. Inverse opals have attracted strong interest in photonic crystal research, due to their full photonic bandgap [39, 40], and are also promising but unexplored materials for phononic experiments.

Complementary to the vertical deposition method a technique for the fabrication of large-area colloidal monolayers has been recently established. This new method itself gives access to highly interesting new materials. Multiple stacks of colloids of various diameters as well as deposition on uneven or curved substrates have been demonstrated. Controlled etching [41] of such a colloidal monolayer allows for the first time the fabrication of large areas of non-close-packed structures. Finally, colloidal monolayers are well known and widely used for surface patterning.

Vertical lifting deposition, colloidal monolayer fabrication and the combination of both are powerful tools in order to rationally design new periodic functional materials with generic possibilities for defect tuning, creation of multilayers, colloidal glasses, non-close-packed materials and inverse opals.

4. The 'music' of the spheres

BLS can be used to measure the resonance modes of dry non-transparent colloidal crystals. Due to the strong elastic form factor of the individual spheres and the large elastic contrast with the surrounding air, the opals show strong multiple scattering. In such samples the inelastic scattering from localized modes leads to incoherent BLS in analogy to the Raman scattering.

Thus BLS can be utilized to analyse the particle eigenfrequencies, describing the spheroidal (i, l) modes, with i as the ith mode of the lth spherical harmonic. The first demonstration of the feasibility of the BLS experiment was shown by Penciu *et al* [42] in the case of dilute suspensions of giant core–shell micelles. A few years later Kuok *et al* [26, 43] have extended this application to closely packed monodisperse silica nanospheres in air. Up to six localized particle eigenmodes have been resolved out of the numerous possible modes, probably due to the weak scattering of moderately compressible silica. In a subsequent study of artificial soft colloidal crystals, composed of monodisperse submicrometre poly(styrene) (PS) spheres [27] with diameter d between 170 and 856 nm, have been investigated. Up to 21 **q**-independent eigenmodes have been resolved.

Figure 2 shows three exemplary BLS spectra from colloidal PS opals with diameters 180, 360 and 550 nm. The resonance frequencies scale with $1/d$ (figure 3), which is in perfect agreement with Lamb's theory [44] and the theoretical predictions based on single-phonon scattering cross-section calculations [45, 46]. In the computations, a plane sound wave propagating in air and impinging upon a single PS sphere was

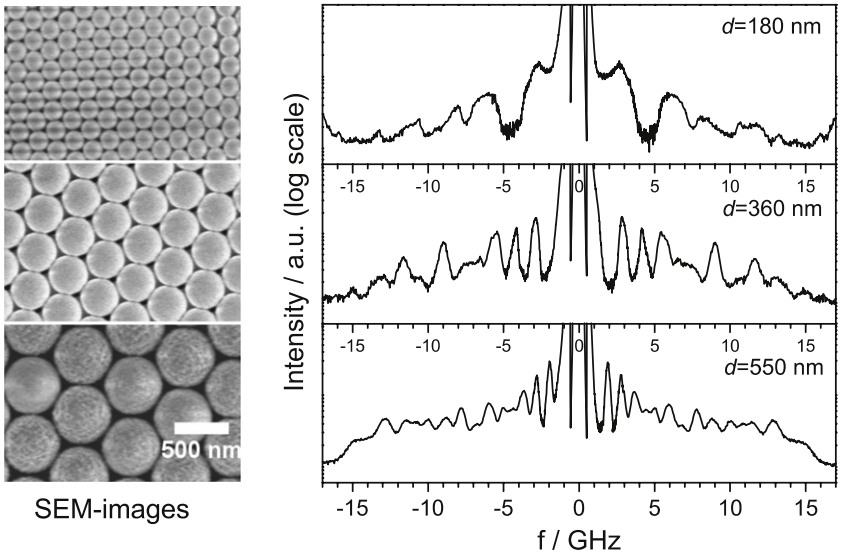

Figure 2. Left: SEM images of colloidal PS crystals with $d = 180$, 360 and 550 nm (top to bottom); right: corresponding **q**-independent BLS eigenmode spectra of the PS opals. To capture all possible vibrations, two spectra recorded at two different free spectral ranges are superimposed. Spectra are recorded at 20° ($q = 0.0041$ nm^{-1}). For the thickest particles ($d = 550$ nm, bottom) there is a clear cutoff bump around 15 GHz, which is the frequency of the acoustic phonon in PS at backscattering geometry.

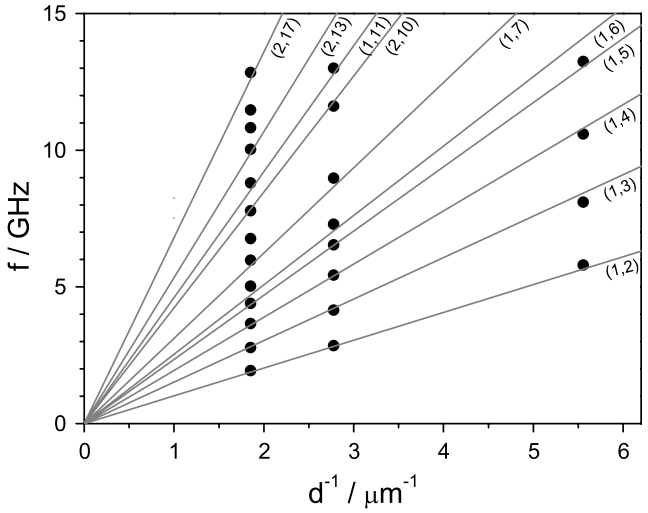

Figure 3. Experimental resonance frequencies of the PS opals from figure 2 (solid symbols) versus the reciprocal particle diameter. The solid lines denote the computed resonance frequencies [27].

considered and, after subtracting the scattering amplitude for a rigid sphere of equal size, the sphere eigenmodes appear as resonance peaks in the plot of scattering cross section versus frequency. Thereby the resonance frequencies $f(i, l)$ can be identified as a mode with angular momentum quantum number l of ith order.

Using the experimental values for the longitudinal sound velocity $c_l = 2350$ ms^{-1}, the transverse sound velocity $c_t = 1210$ ms^{-1} and mass density $\rho = 1050$ kg m^{-3} of bulk PS, all resolved frequencies are quantitatively captured within 3% with no adjustable parameter. The product of frequency and diameter is obtained to be a constant for every mode, as is indicated by the solid lines in figure 3, which represent the computed modes (i, l). It is shown that the first modes are the same for all samples with the (1, 2) mode being the lowest and most intense one.

From the longitudinal and transversal sound velocities the elastic constants are directly accessible. These are the Poisson ratio $\sigma = (c_l^2 - 2c_t^2)/(2(c_l^2 - c_t^2))$, the Young modulus $E = \rho c_l^2(1 + \sigma)(1 - 2\sigma)/(1 - \sigma)$ and the shear modulus $G = \rho c_t^2$ [47]. Additionally to the elastic constants, even more information can be extracted from these spectra. The peculiar lineshape can be regarded as a sensitive index of the particle size distribution. In particular for the (1, 2) modes (figure 4 in [27]), the experimental lineshape (after deconvolution with the instrument function) can be represented by a convolution of a Lorentzian line and a Gaussian distribution function of the particle size with their variance as the only adjustable parameter besides the amplitude. In conformity with the analysis of the SEM pictures all investigated colloidal samples are found to be quite monodisperse. For the largest particle size in figure 2 (or figure 2 in [27]) there is clearly a kind of cutoff frequency at about 14–15 GHz, after which the scattering intensity decreases rapidly towards zero.

Because of strong multiple scattering, **q** is not defined. The highest frequency contribution corresponds to the acoustic phonon in bulk PS under backscattering conditions, i.e. $q_{BS} = 4\pi n/\lambda_0$. Using $n = 1.59$ for the refractive index of PS and for the laser wavelength $\lambda_0 = 532$ nm, $q_{BS} = 0.0376$ nm^{-1} and hence a cutoff frequency for the longitudinal acoustic phonon ($c_l = 2350$ ms^{-1}) is indeed expected at 14.05 GHz.

A more detailed theoretical treatment of the Brillouin and Raman scattering from the acoustic vibrations of spherical particles with diameters of the order of magnitude of the wavelength of light was presented very recently by Montagna [48]. While for very small particles ($qR \ll 1$, with $R = d/2$) only the 'Raman term' that originates either from local field changes due to dipole-induced dipoles or

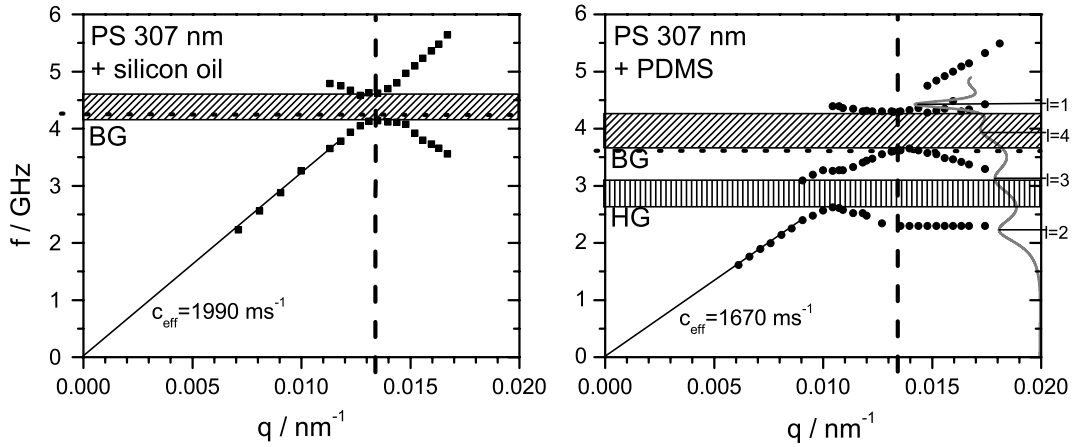

Figure 4. The dispersion relations of a colloidal PS ($d = 307$ nm) opal infiltrated with silicon oil (left, see also [17]) and with PDMS (right, see also [25]) in the Γ–M direction of the fcc crystals are compared. In both spectra there is a clear BG (diagonal pattern). The dashed lines indicate the Γ–M distance in the reciprocal space, hence the edge of the first Brillouin zone ($q_{BZ} = (3/2)^{3/2}\pi/\sqrt{2}d$ or $q_{BZ} = 0.0133$ nm^{-1} for $d = 307$ nm). The dotted lines denote the frequencies that correspond to q_{BZ} ($c_{eff}q_{BZ}/2\pi$). For the opal infiltrated with PDMS a HG (vertical pattern) appears, too. The grey curve on the right side represents the theoretically calculated DOS.

from electronic polarizability changes with the change of the atomic distances is important, for particles with diameters $d \sim \lambda_0$ the 'Brillouin term' also becomes important. The latter comes from the polarization fluctuations caused by spatial displacement of scatterers by acoustic vibrations. Detailed calculations are performed, which show that for a given l the intensity of a resonance mode with a certain i strongly depends on qR, hence on the particle size. However, a direct comparison with the experiment is not straightforward due to the ill-defined **q**. Nevertheless, it is pointed out that for larger particle sizes the range of qR also increases ($0 \leqslant qR \leqslant q_{BS}R$). In a given range of qR only the mode's resonance frequencies that are close to that of the acoustic phonon in the bulk, i.e. $\omega \approx qc_l$, contribute considerably to the Brillouin scattering. The total number of modes with higher i and l that have their intensity maximum in the larger qR range also increases. This rationalizes the observation of the highest number of modes for the better-formed cutoff for the largest particles in figure 2.

An additional application of the detection of the particle eigenfrequencies via BLS with technological relevance was the determination of the mechanical properties of spherical glassy $CaCO_3$ particles [47]. The particles with mono-modal size distributions and diameters in the range between 400 and 1500 nm were made from amorphous $CaCO_3$, with unknown elastic properties as yet. Eigenmode acoustic spectra of the spheres were recorded and six or seven resonance modes could be resolved. By calculating c_l from the cutoff frequencies and taking c_t and the density ρ as floating fit parameters, all signals could be assigned to the vibrational eigenmodes and a very good agreement between theory and experiment was achieved. From the obtained values for c_l, c_t and ρ the Poisson ratio σ, Young modulus E and shear modulus G were then reported.

5. Phononic bandgaps

To measure the phononic dispersion relation of colloidal crystals by BLS, the strong multiple scattering should be overcome. This is achieved by infiltration of the dry opals by a fluid with refractive index close to that of the colloidal spheres. For poly(methylmethacrylate) (PMMA, $n = 1.49$) or PS ($n = 1.59$) colloids, for example silicon oil ($n = 1.45$) or liquid poly(dimethylsiloxane) (PDMS, $n = 1.41$), are suitable infiltration liquids. Using such 'wet' colloidal crystals, the first experimental access to the phononic band diagram along high symmetry directions in submicrometre artificial crystals was recently reported [17] leading to the observation of phononic bandgaps in the GHz range. Till then, only sonic and ultrasonic crystals had been investigated by other techniques, mostly by sonic and ultrasonic transmission experiments or by a special video spectroscopy method applied to 2D [49] and 3D [50] experiments. The observation of a hypersonic bandgap in a 2D hypersonic phononic crystal by BLS was subsequently reported [51].

The nature of the observed bandgaps is clearly that of a 'Bragg gap' (BG). A BG exists due to annihilation of the incident mechanical wave and the waves scattered on the individual spheres in the crystal. To create a bandgap, the periodic structure length in the crystal must be of the order of the relevant phonon wavelength. If the phonon wavelength and the distance between the crystal planes in the direction of the phonon propagation become equal, the scattered mechanical waves interfere constructively and the energy of the incident wave is reflected back, opening a phononic gap.

FCC crystals of submicron PS spheres are prepared by vertical lifting deposition. After infiltration with PDMS, the dispersion relation, $f(q)$, was recorded by angle-dependent BLS measurements along high-symmetry directions in the reciprocal space. As shown in figure 4 at low q's the dispersion relation is that of mechanical waves travelling through a homogeneous medium with an effective sound velocity, i.e.

$$\omega = 2\pi f = c_{eff}q. \tag{1}$$

As q reaches the edge of the first Brillouin zone (BZ) at $q_{BZ} = (3/2)^{3/2}\pi/(\sqrt{2}d)$ in the probed Γ–M direction, the fulfilment

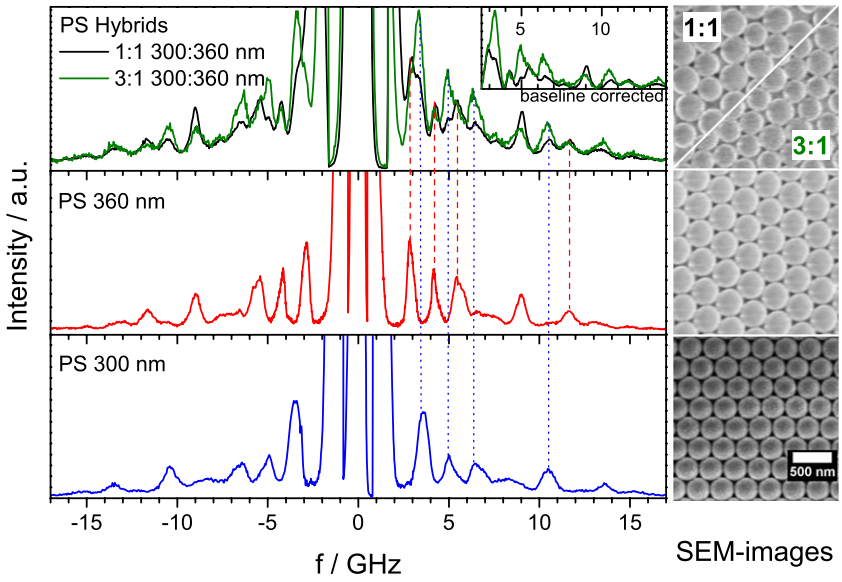

Figure 5. Left: eigenmode acoustic spectra of the PS opals with $d = 300$ nm (blue), $d = 360$ nm (red) and the symmetric PS hybrids 1:1/3:1 300 nm:360 nm (black/green)(bottom to top). The vertical lines (dotted for $d = 300$ nm, dashed for $d = 360$ nm) denote some exemplary eigenmodes appearing in the opals and in the hybrids. In the top right corner the Stokes sides of the hybrids' spectra are compared after baseline correction to better visualize the influence of the composition on the relative intensity of the individual signals. Right: corresponding SEM images of opals and hybrids shown on the left side.

of the Bragg condition leads to a gap opening. Accordingly, the frequency of the observed gap [17] is

$$f = q_{\mathrm{BZ}} c_{\mathrm{eff}}/2\pi. \tag{2}$$

The position of the gap can be widely tuned by changing the lattice parameters of the hypersonic phononic crystal due to the linear dependence of the gap frequency from the inverse diameter.

The width of the BG increases with elastic mismatch between the spheres and the infiltrated liquid. In fact, the width of the gap in the wet PS opals systematically increases when the infiltrated liquid changes from glycerine ($c_{\mathrm{l}} \sim 2200$ ms^{-1}) to silicon oil ($c_{\mathrm{l}} = 1400$ ms^{-1}) and to PDMS ($c_{\mathrm{l}} = 1050$ ms^{-1}). According to the results of effective medium theory [52, 53] the value of c_{eff} lies in between the components' individual sound velocities. It is noteworthy that the calculation of effective sound velocities following the approach of Gaunaurd and Wertman [53] tends to result in moderately but certainly too small values compared with the experiment: actually the deviations are smaller than 10%.

Very recently [25] we demonstrated the experimental realization of an additional gap besides the BG, the so-called hybridization gap (HG). This HG originates from the interaction of the band of quadrupole particle eigenmodes with the band of the effective medium. This kind of gap opens up from level repulsion when two bands of the same symmetry cross each other (in analogy to the linear combination of atomic orbitals) [54]. In this case, the involved bands are the acoustic field of the extended states in the effective medium and the bands from the multipole modes of the interacting spherical particles, which can be treated as local resonant elements.

The first hint of this gap was found in BLS experiments in colloidal suspensions [55, 56], but a clear demonstration, assignment and the concurrent observation along with the BG was just reported [25] in the case of PS and PMMA wet opals infiltrated with PDMS. It should be mentioned that infiltration with silicon oil does not promote the HG and only the BG is observed (figure 4).

In order to prove whether the newly observed gap relates to the theoretically predicted HG, we performed density-of-states (DOS) calculations [46] for the acoustic DOS in the infiltrated systems. Figure 4 shows the full dispersion relation of a 307 nm PS opal infiltrated with PDMS along with the corresponding DOS [25]. It is conspicuous that the opening of the HG is next to the position of the calculated $f(1, 2)$, the lowest modes in the wet systems as well as in the dry systems shown above. Indeed, for high q's up to three localized modes appear that seem to correspond to the higher particle resonances. This suggests that these modes are localized mostly inside each colloidal particle [45].

6. Hybrids

The assignment of the two phononic gaps is also corroborated by their sensitivity on the disorder. In this context, we prepared non-crystalline colloidal films by vertical lifting deposition of 'hybrids', binary mixtures consisting of an equal number of two PS spheres with different diameters ($d = 300$ and 360 nm). The size polydispersity is then artificially increased and no crystallization takes place, which is affirmed by SEM pictures. The eigenmode acoustic spectra of these dry 'hybrid' films and the dispersion relations in their infiltrated counterparts were measured by BLS. The eigenmode spectrum of the 1:1 300:360 nm hybrid is shown in figure 5 along with the eigenmode spectra of the individual one-component opals. Interestingly, the spectrum of the hybrid is a superposition

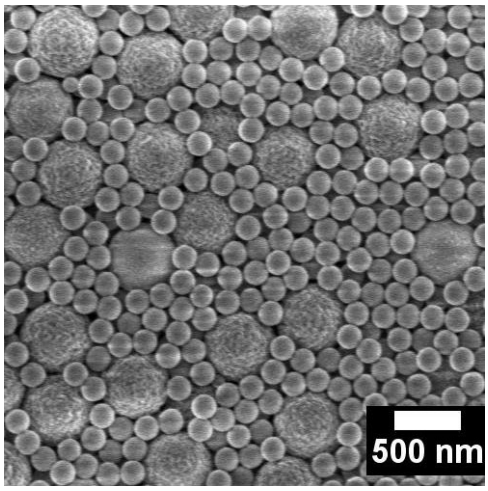

Figure 6. SEM image of the 9:1 180:550 nm PS hybrid.

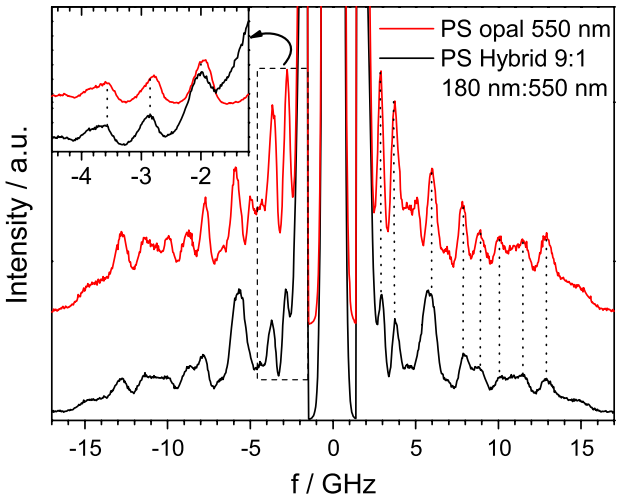

Figure 7. Comparison between the eigenmode acoustic spectra of the 550 nm PS single opal and the highly asymmetric 9:1 180 nm:550 nm PS hybrid.

of the individual opals as is indicated by the vertical lines denoting some exemplary resonance frequencies either from the small or the large spheres. Moreover, we prepared hybrids of different relative ratios of the constituent spheres. The intensity of the signals originating from a particular particle size relates to its composition in the mixture. In figure 5 we demonstrate this linear composition dependence by superimposing the spectrum of the 1:1 300 nm:360 nm hybrid with the spectrum of a 3:1 300 nm:360 nm hybrid, normalized to the peak intensity in the 360 nm spheres. For clarity a baseline correction was introduced into the Stokes side of the hybrids (inset to figure 5).

Apparently, but somewhat counterintuitively, the contact between the spheres does not influence their eigenmodes—at least for non-infiltrated dry films. We also examined only partially ordered samples of monodisperse nanospheres prepared by dropping a few drops of the suspension of the spheres onto a glass substrate. In spite of the lack of any order, the eigenmode spectra of these samples are indistinguishable from those of the colloidal crystals. To undermine the contact argument, the consistency of the spectra's features would be based upon the small differences between the opals and the hybrids for 300 and 360 nm PS spheres. We also investigated very asymmetric hybrids with a nine to one number ratio of 180 and 550 nm PS beads. While for every dense packing of spheres the number of neighbouring spheres, and hence the contact points as indicated by the SEM images, is twelve, this mean number is different for the random packed hybrids depending on their size disparity and their number ratio. For example, in the SEM image for a 9:1 180 nm:550 nm hybrid in figure 6, the number of next neighbours of the large spheres is increased dramatically by small beads that accumulated around the bigger spheres. However, even in this extreme case, the resonances from the 550 nm spheres are virtually unaltered as demonstrated in the spectra of figure 7. A careful inspection, however, of the two lowest frequencies reveals a very small shift of the hybrid resonance modes towards higher frequencies as is shown in the inset of figure 7 for the Stokes sides of the spectra, though the observed effect is subtle (∼4% frequency shift) but significant. In this context it is noteworthy to mention that in figure 3 of [57], Li *et al* compare the BLS spectra from a 320 nm silica artificial opal and from a single sphere of the same kind, measured by a micro-Brillouin light scattering set-up. In this figure it seems as if there is a shift between single spheres and opal. Interestingly, the authors describe only the broadening in the opal due to the polydispersity.

The effect of the disorder on the dispersion relation of our PS hybrids after infiltration is shown in figure 8 (see also figure 3 in [25]). Here, we compare the dispersion relation of the 9:1 260 nm:360 nm hybrid with those of the 260 nm opal, both infiltrated with PDMS. The most striking result is that the HG is robust against structural disorder whereas the BG vanishes. This is in agreement with the nature of the gaps, because the BG is an effect of the crystal structure while the sphere resonances that excite the opening of the HG are unchanged by the arrangement of the spheres. The absence of an influence of disorder also means that the HG is independent of crystallographic directions and hence omnidirectional, i.e. the HG is consequently an absolute bandgap.

The width of the HG in the wet opal is found to be broader than for the hybrid colloidal film. For infiltrated hybrids, the interactions between the vibrations of the individual spheres are expected to be stronger compared to the dry opals. However, to elucidate this density effect on the HG, a broad range of different PS hybrids should be examined.

7. Conclusions and outlook

Colloidal self-assembly by vertical lifting is a potent method to create and design artificial submicron periodic structures of hard (e.g. SiO_2) and soft (polymers) colloidal particles. The fabrication of high quality crystals as well as the creation of artificial glasses by the introduction of structural disorder is possible. Such samples have spatial dimensions of their components of the order of the wavelength of visible light,

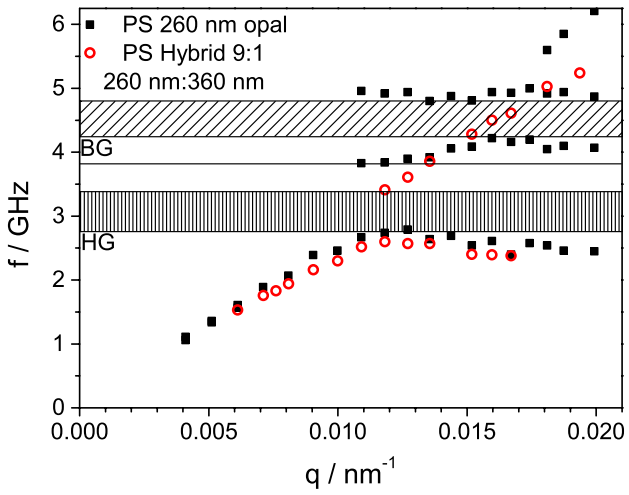

Figure 8. Dispersion relations of a PS hybrid 9:1 260 nm:360 nm (red points) in comparison with that of the pure PS 260 nm opal (black squares), both infiltrated with PDMS. The HG (vertical pattern) appears for both samples whereas the BG (diagonal pattern) is deleted in the hybrid.

hence they act as artificial opals. In addition, they show interesting phononic properties in the hypersonic (GHz) range.

BLS is found to be a powerful technique to measure the elastic properties of nanostructured materials at hypersonic frequencies. In the case of dry non-transparent colloidal samples, BLS measures **q**-independent localized modes of the individual spheres. In particular, for soft spheres these spectra are found to be richer with increasing diameter. This finding is explained by theoretical and geometrical considerations. Nearly all predicted modes (especially those that appear at frequencies significantly below that of the acoustic phonon in the backscattering case) are found experimentally and assigned to their corresponding spheroidal eigenmodes. In contrast to other studies [26] and theoretical expectations [48] torsional ($l = 0$) modes are not observed. The analysis of the eigenmode spectra yields the longitudinal c_l and transverse sound velocity c_t, allowing the calculation of the Young and shear elastic moduli at the nanoscale. Additionally, the analysis of the lineshape can provide information on the size polydispersity.

Utilizing several 'hybrid' mixtures, we show that the eigenfrequencies do not depend on the crystalline order or on the kind and number of the neighbouring spheres. Only in the extreme case of dilute large spheres in a sea of small spheres was a small blue shift observed.

By infiltration of the dry samples with a liquid close to optical matching, we can overcome the multiple light scattering. BLS can be used to record directly the dispersion relations that led to the first demonstration of a distinct hypersonic Bragg gap. So far phononic gaps were observed in much larger structures and hence frequencies in the sonic and ultrasonic range. The resonant character of the particles was realized to demonstrate the presence of an additional bandgap—the hybridization gap, theoretically predicted for some time. This HG originates from the interaction of the acoustic band of the effective medium and bands from the multipole modes of the individual particles. For our materials, the HG is found to open up at frequencies below that of the Bragg gap.

These phononic materials might have interesting potential applications starting with the obvious use as acoustic shields or vibration isolators. However, for most practical applications, gap frequencies in the range of sonics or ultrasonics seem to be of higher interest than those in the hypersonic range. On the other hand, if the blocked phonon's wavelength is comparable to the structure dimensions, i.e. $\lambda \sim d$, then the structure's components for ultrasonic devices must be near to the mm range and even larger to stop sound between kHz and Hz. The ultimate goal would be to create materials which can realize gaps at wavelengths much larger than the inherent length scale of the gap material ($\lambda \gg d$). Ping Sheng and coworkers [8] demonstrated an approach going in this direction. They prepared locally resonant sonic materials by combining a spherical lead core and a silicone rubber coating in the millimetre size range and building up a crystal out of these. The resulted superstructure exhibits a bandgap around 400 Hz, which corresponds to a wavelength two orders of magnitude bigger than the diameter of the spheres. Like HG the explanation is due to localized modes mostly in the soft shells. Advances in colloidal science can be utilized to provide materials with new functions. For example, core–shell particles with varying composition, hybrid materials or materials with even hierarchical order can allow tailoring the phononic properties of small but smart materials to frequencies, where a broad range of applications is conceivable.

When we turn our attention back to the manipulation of the phonon flow in the GHz range, hypersonic phononic materials hold promise to control heat flow. If we will control the flow of elastic energy by building phonon guiding devices in full analogy to the lossless light guidance in photonics or by building devices with a strong anisotropy of phonon transmission, we can also attain new knowledge in advanced heat management. In this direction, colloidal science could offer new materials, e.g. multilayer structures with different particle sizes in each structure, that could split and direct the elastic energy. Other analogies to photonics, e.g. acoustic superlenses, already exist but still impose challenges for high frequency acoustics. It should be mentioned that hypersonic phononics can simultaneously act as photonics for wavelengths in the visible spectrum, allowing for acousto-optical coupling [58].

In parallel to the development of materials with new phononic functions, there is also a need for new experimental techniques to measure the band diagrams of non-transparent structures also exhibiting strong phononic gaps. BLS is a powerful technique for transparent samples with serious shortcomings in opaque systems such as dry opals and in measuring hypersonic transmission spectra. The main problem is the availability of a selective and continuous generation of phonons in the GHz range.

Acknowledgments

Partial support from EC (SoftComp) is gratefully acknowledged. MR thanks the FCI for the Kekulé mobility scholarship.

We thank Professor N Stefanou and Dr R Sainidou for fruitful collaboration.

References

[1] Yablonovitch E 1987 *Phys. Rev. Lett.* **58** 2059–62
[2] John S 1987 *Phys. Rev. Lett.* **58** 2486–9
[3] Joannopoulos J D, Johnson S G, Winn J N and Meade R D 2008 *Photonic Crystals: Molding the Flow of Light* 2nd edn (Princeton, NJ: Princeton University Press)
[4] Sigalas M and Economou E N 1993 *Solid State Commun.* **86** 141–3
[5] Kushwaha M S, Halevi P, Dobrzynski L and Djafari-Rouhani B 1993 *Phys. Rev. Lett.* **71** 2022–5
[6] Martinez-Salazar R, Sancho J, Sanchez J V, Gomez V, Llinares J and Meseguer F 1995 *Nature* **378** 241
[7] Montero de Espinosa F R, Jimnez E and Torres M 1998 *Phys. Rev. Lett.* **80** 1208
[8] Liu Z Y, Zhang X X, Mao Y W, Zhu Y Y, Yang Z Y, Chan C T and Sheng P 2000 *Science* **289** 1734–6
[9] Liu Z Y, Chan C T, Sheng P, Goertzen A L and Page J H 2000 *Phys. Rev.* B **62** 2446–57
[10] Vasseur J O, Deymier P A, Chenni B, Djafari-Rouhani B, Dobrzynski L and Prevost D 2001 *Phys. Rev. Lett.* **86** 3012–5
[11] Sheng P and Chan C T 2005 *Z. Kristallogr.* **220** 757–64
[12] Gorishnyy T, Maldovan M, Ullal C and Thomas E 2005 *Phys. World* **18** 24–9
[13] Sanchez-Perez J V, Caballero D, Martinez-Sala R, Rubio C, Sanchez-Dehesa J, Meseguer F, Llinares J and Galvez F 1998 *Phys. Rev. Lett.* **80** 5325–8
[14] Dobrzynski L, Djafari-Rouhani B, Akjouj A, Vasseur J O and Zemmouri J 1999 *Europhys. Lett.* **46** 467–70
[15] Lu M H, Zhang C, Feng L, Zhao J, Chen Y F, Mao Y W, Zi J, Zhu Y Y, Zhu S N and Ming N B 2007 *Nat. Mater.* **6** 744–8
[16] Lin K H, Lai C M, Pan C C, Chyi J I, Shi J W, Sun S Z, Chang C F and Sun C K 2007 *Nature Nanotech.* **2** 704–8
[17] Cheng W, Wang J J, Jonas U, Fytas G and Stefanou N 2006 *Nat. Mater.* **5** 830–6
[18] Gorishnyy T, Ullal C K, Maldovan M, Fytas G and Thomas E L 2005 *Phys. Rev. Lett.* **94** 115501
[19] Campbell M, Sharp D N, Harrison M T, Denning R G and Turberfield A J 2000 *Nature* **404** 53–6
[20] Deubel M, Wegener M, Kaso A and John S 2004 *Appl. Phys. Lett.* **85** 1895–7
[21] Cumpston B H, Ananthavel S P, Barlow S, Dyer D L, Ehrlich J E, Erskine L L, Heikal A A, Kuebler S M, Lee I Y S, McCord-Maughon D, Qin J, Rockel H, Rumi M, Wu X L, Marder S R and Perry J W 1999 *Nature* **398** 51–4
[22] Xia Y N, Gates B, Yin Y D and Lu Y 2000 *Adv. Mater.* **12** 693–713
[23] Wang J, Ahl S, Li Q, Kreiter M, Neumann T, Burkert K, Knoll W and Jonas U 2008 *J. Mater. Chem.* **18** 981–8
[24] Wang J J, Li Q, Knoll W and Jonas U 2006 *J. Am. Chem. Soc.* **128** 15606–7
[25] Still T, Cheng W, Retsch M, Sainidou R, Wang J, Jonas U, Stefanou N and Fytas G 2008 *Phys. Rev. Lett.* **100** 194301
[26] Kuok M H, Lim H S, Ng S C, Liu N N and Wang Z K 2003 *Phys. Rev. Lett.* **90** 255502
[27] Cheng W, Wang J J, Jonas U, Steffen W, Fytas G, Penciu R S and Economou E N 2005 *J. Chem. Phys.* **123** 121104
[28] Davis K E, Russel W B and Glantschnig W J 1989 *Science* **247** 507
[29] Trau M, Saville D A and Aksay I A 1996 *Science* **272** 706
[30] Jiang P, Bertone J F, Hwang K S and Colvin V L 1999 *Chem. Mater.* **11** 2132–40
[31] Gu Z Z, Fujishima A and Sato O 2002 *Chem. Mater.* **14** 760–5
[32] Fustin C A, Glasser G, Spiess H W and Jonas U 2004 *Langmuir* **20** 9114–23
[33] Denkov N, Velev O, Kralchevski P, Ivanov I, Yoshimura H and Nagayama K 1992 *Langmuir* **8** 3183–90
[34] Tommaseo G, Petekidis G, Steffen W, Fytas G, Schofield A B and Stefanou N 2007 *J. Chem. Phys.* **126** 014707
[35] Fustin C A, Glasser G, Spiess H W and Jonas U 2003 *Adv. Mater.* **15** 1025–8
[36] Pusey P N and van Megen W 1987 *Phys. Rev. Lett.* **59** 2083
[37] García P D, Sapienza R, Blanco A and López C 2007 *Adv. Mater.* **19** 2597–602
[38] Zakhidov A A, Baughman R H, Iqbal Z, Cui C, Khayrullin I, Dantas S O, Marti J and Ralchenko V G 1998 *Science* **282** 897–901
[39] Li Z Y and Zhang Z Q 2000 *Phys. Rev.* B **62** 1516
[40] Li Z Y and Zhang Z Q 2001 *Adv. Mater.* **13** 433–6
[41] Haginoya C, Ishibashi M and Koike K 1997 *Appl. Phys. Lett.* **71** 2934–6
[42] Penciu R S, Fytas G, Economou E N, Steffen W and Yannopoulos S N 2000 *Phys. Rev. Lett.* **85** 4622
[43] Kuok M H, Lim H S, Ng S C, Liu N N and Wang Z K 2003 *Phys. Rev. Lett.* **91** 149901
[44] Lamb H 1882 *Proc. London Math. Soc.* **s1-13** 189
[45] Penciu R S, Kriegs H, Petekidis G, Fytas G and Economou E N 2003 *J. Chem. Phys.* **118** 5224–40
[46] Sainidou R, Stefanou N, Psarobas I E and Modinos A 2005 *Z. Kristallogr.* **220** 848–58
[47] Faatz M, Cheng W, Wegner G, Fytas G, Penciu R S and Economou E N 2005 *Langmuir* **21** 6666–8
[48] Montagna M 2008 *Phys. Rev.* B **77** 045418
[49] Baumgartl J, Zvyagolskaya M and Bechinger C 2007 *Phys. Rev. Lett.* **99** 205503
[50] Reinke D, Stark H, von Grunberg H H, Schofield A B, Maret G and Gasser U 2007 *Phys. Rev. Lett.* **98** 038301
[51] Gorishnyy T, Jang J H, Koh C and Thomas E L 2007 *Appl. Phys. Lett.* **91** 121915
[52] Harker A H and Temple J A G 1988 *J. Phys. D: Appl. Phys.* **21** 1576–88
[53] Gaunaurd G C and Wertman W 1989 *J. Acoust. Soc. Am.* **85** 541–54
[54] Kafesaki M and Economou E N 1995 *Phys. Rev.* B **52** 13317
[55] Liu J, Ye L, Weitz D A and Ping S 1990 *Phys. Rev. Lett.* **65** 2602–5
[56] Jing X, Sheng P and Zhou M 1991 *Phys. Rev. Lett.* **66** 1240
[57] Li Y, Lim H S, Ng S C, Wang Z K, Kuok M H, Vekris E, Kitaev V, Peiris F C and Ozin G A 2006 *Appl. Phys. Lett.* **88** 023112
[58] Maldovan M and Thomas E L 2006 *Appl. Phys. Lett.* **88** 251907